SEMARAK ILMU PUBLISHING

Journal of Advanced Research in Fluid Mechanics and Thermal Sciences

Journal homepage:
https://semarakilmu.com.my/journals/index.php/fluid_mechanics_thermal_sciences/index
ISSN: 2289-7879

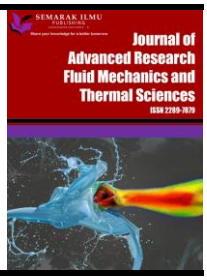

Heat Transfer in Hartmann Flow of Hybrid Nano-Jeffrey Fluid with Heat Absorption and Thermal Radiation Impact

Nor Athirah Mohd Zin[1,*], Siti Nur Alwani Salleh[1], Ahmad Qushairi Mohamad[2], Mohd Rijal Ilias[3], Ilyas Khan[4]

[1] Mathematical Sciences Studies, College of Computing, Informatics and Mathematics, Universiti Teknologi MARA (UiTM), Kedah Branch, Sungai Petani Campus, 08400, Merbok, Kedah, Malaysia
[2] Department of Mathematical Sciences, Faculty of Science, Universiti Teknologi Malaysia, 81310, Johor Bahru, Johor, Malaysia
[3] School of Mathematical Sciences, College of Computing, Informatics and Mathematics, Universiti Teknologi MARA, 40450 Shah Alam, Selangor, Malaysia
[4] Department of Mathematics, College of Science Al-Zulfi, Majmaah University, Al-Majmaah,11952, Saudi Arabia

ARTICLE INFO

Article history:
Received 23 August 2023
Received in revised form 9 November 2023
Accepted 20 November 2023
Available online 15 December 2023

Keywords:
Unsteady Jeffrey hybrid nanofluid; magnetic field; radiation; heat absorption; Laplace transform

ABSTRACT

In this study, we examine how heat radiation and absorption affect the flow of Jeffrey fluid across an infinite vertical plate in an unsteady magnetohydrodynamic (MHD) free convection flow. We use alumina (Al_2O_3) and copper (Cu) nanoparticles in water assuming it as a base fluid. The problem is solved, and exact solutions are obtained using the Laplace transform method. For embedded parameters like radiation parameter, heat absorption parameter, Hartmann number, Grashof number, material parameter of Jeffrey fluid, volume fraction of hybrid nanofluid, time, and Prandtl number, results of velocity and temperature distributions are visually displayed. It is clear from the results that while raising the heat absorption parameter and Prandtl number causes a decrease in the velocity and temperature profiles whereas increasing radiation parameter and Grashof Number increases the hybrid nanofluid velocity. The resulting analytical solution is then verified by comparing it to the results of the earlier investigation and is determined to be in excellent accord. This outcome may be used in a number of nanofluid cooling systems. This research might serve as a reference for other numerical and experimental studies as well as a manual for several industries because the answers are established in an analytical form.

1. Introduction

Due to the limited capabilities of conventional base fluids like ethylene glycol, engine oil, and water, are not sufficient to address today's needs, thus, an advanced form of high-potential heat transport fluid namely nanofluid is introduced and launched in the industrial area. Nanofluid is formed by adding some nanoparticles whose size of less than 100 nm in conventional base fluids [1]. Nanofluid shows better performance in heat transfer than regular fluids. Many investigations on nanofluid flow with various physical situations have been done by several authors; Hanif [2], Hanif

* *Corresponding author.*
E-mail address: athirahmz@uitm.edu.my

https://doi.org/10.37934/arfmts.112.1.3861

and Shafie [3,4], Saeed *et al.,* [5], Sharma *et al.,* [6,7], and Mishra *et al.,* [8]. A major requirement for today's industry is the existence of systems or applications that allow heat transfer to occur more quickly. A lot of articles report that new hybrid nanoparticles may enhance the heat transfer rate compared to regular nanofluid [9]. The special behaviors of the hybrid nanofluid are its thermal conductivity and viscosity increase with increasing particle concentration in the base fluids. In recent years, hybrid nanofluids gained great importance in several industrial and technological processes such as electronic cooling, transportation, solar energy, automobiles, smart computers, catalysis, microfluidics, and biomedicine [10-13]. Driven by these important applications, many studies have been performed to analyze the boundary layer flow of a hybrid nanofluid. Salleh *et al.,* [14] examined the stability of the dual solutions obtained for the hybrid nanofluid flow past a moving thin needle. Hussain *et al.,* [15] performed the flow of a hybrid nanofluid in the presence of the convective condition using an exponentially stretchable rotating surface. The influence of Friedrich shear stress, hybrid nanoparticles, and Cattaneo heat flux on the characteristic of the flow and heat transfer of Maxwell hybrid nanofluid is studied by Hanif and Shafie [16]. Later, Dinarvand *et al.,* [17] carried out an analysis of mixed convection flow over a shrinking and porous surface of thermomicropolar silver and graphene nanoparticles using the mass-based hybrid nanofluid model. A considerable amount of previous research on hybrid nanofluid under various situations has been successfully reported [18-24].

The main concern in the study of non-Newtonian fluids in the last few years is due to their practical usage in industry and technology. Several examples of non-Newtonian fluids are blood, dilute polymer solution, honey, gel, and many others. The main aspect of non-Newtonian fluid's importance is that it possesses nonlinear rheological properties [25-27]. Since many applications (geophysics, bioscience, cosmetics, drying of paper, food processing, chemical plastic production, and petroleum industries) involved rheological problems, many flow models have been proposed to interpret non-Newtonian fluids' behaviour [28,29]. The best solution to interpret that behaviour is by using the Jeffrey fluid model due to its simplicity. Among the non-Newtonian fluid models, the Jeffrey fluid model is often used because its constitutive equations can be reduced to the Newtonian model as a special case. Jeffrey fluid can describe the stress relaxation properties and relaxation time of non-Newtonian fluids, which normal fluids cannot describe. In recent years, many authors have investigated several studies of the Jeffrey fluid under different conditions. For instance, Sharma *et al.,* [30] analyzed the electromagnetohydrodynamic Jeffrey fluid flow past a vertical nonlinear stretching surface of variable thickness. In their study, they analyzed the effects of heat and mass transfer by using several source terms namely, thermophoresis, Brownian motion, Ohmic heating, viscous dissipation, exponential heat source, thermal heat source, and activation energy. Awais *et al.,* [31] investigated the impact of Hall current on magnetohydrodynamic flow with Jeffrey fluid adjacent to a nonlinear stretching plate with variable thickness. Hussain *et al.,* [32] carried out an investigation to analyse the Cattaneo–Christov heat flux in Jeffrey fluid flow in the presence of a heat source past a stretchable cylinder. They conclude that higher values of Deborah number in terms of relaxation time and ratio parameter diminishes the magnitude of the drag coefficient, while the opposite effect is noticed for larger Deborah number in terms of retardation time and curvature parameter. Recently, Kumar *et al.,* [33] analyzed the effects of Joule heating, viscous dissipation, exponential heat source, and Arrhenius activation energy on an electromagnetohydrodynamic Cu-polyvinyl alcohol/water Jeffrey nanofluid flow. It is found that the heat transfer rate augments with an increase in the thermophoresis diffusion and electric field parameters, while it diminishes with an increase in an exponential heat source parameter. More articles on Jeffrey fluid flow are available in the recent literature [34-36].

The consideration of the magnetic field in the flow plays a significant role in various fields such as medical, chemical, biological, and mechanical. For example, magnetohydrodynamics (MHD) power generators, MHD flow meters, loudspeaker fabrication, sink-float separation, magnetic resonance image, device sterilization, sealing of materials, and granular insulation. In the area of medicine, magnets are used to create three-dimensional images of diagnostic and anatomical importance from nuclear magnetic resonance signals. Due to these important applications, a lot of research has been done by many authors. Krishna *et al.,* [37] studied the peristaltic magnetohydrodynamic flow of a Jeffrey fluid past a porous medium in a vertical echelon by considering the impact of uniform transverse magnetic field as well as Hall current. A year later, Krishna *et al.,* [38] furthered their study by examining the influence of Joule, Soret, and Hall currents on MHD rotating mixed convection flow adjacent to an infinite porous surface. Inspired by the previously published paper, a lot of investigations have been carried out to focus on the magnetohydrodynamic [39-42]. Very recently, Reddy *et al.,* [43] examined the influence of the porosity on unsteady MHD mixed convection stagnation point flow with radiation and viscous dissipation, meanwhile, Sharma *et al.,* [44] analyzed the influence of porosity, radiation, and viscous dissipation on unsteady MHD mixed convection flow at the stagnation point.

Other than that, the researchers are devoted to discovering new energy technologies and energy resources. The analysis of radiative heat flux is highly important in space technology and processes that demand high temperatures [45]. There are numerous applications of radiation effects such as electricity generation, astrophysical flows, and solar power technologies. The consideration of radiation in the energy equation leads to a highly nonlinear partial differential equation. A lot of research has been conducted to analyze the radiation effect on the flow. Roşca *et al.,* [46] discussed the theoretical and numerical outcomes for an axisymmetric hybrid nanofluid flow under the influence of radiation past a stretching/shrinking plate. It is noticed from their study that the addition of radiation effect enhances the fluid temperature. The variation of the energy dissipation, diameter of nanoparticles, and mass flux caused by the temperature gradient in convective radiation of the fluid, Darcy-Forchheimer model, and heat source has been investigated by Ali *et al.,* [47] considering cylindrical surface. Besides that, Bejawada *et al.,* [48] examined computationally the effect of thermal radiation, heat source and chemical reaction on magnetohydrodynamic Casson fluid flow with velocity slip past a nonlinear inclined stretchable sheet in a Forchheimer porous medium. They noted that the presence of radiation in the flow decreases the plate temperature. Recently, several researchers have conducted various versions of these effects on flow fields [49-53].

From the published literature it is found that no study on Jeffrey nanofluid with hybrid nanoparticles is performed under the imposed constraints. Hence to fill this gap, this study is carried out. More exactly, in this work we have explored the analytical solutions of MHD Jeffrey hybrid nanofluid flow under the effects of thermal radiation, heat absorption, and magnetic field. Two different kinds of nanoparticles, namely, alumina and copper are taken into consideration. To the best of knowledge, this problem has not been reported in recent literature yet. Further studies on this topic should be conducted by more researchers. In this work, a set of appropriate dimensionless variables are applied to reduce the partial differential equations into a non-dimensional form. The analytical solutions for these governing equations are computed by the Laplace transform method. Some interesting results of velocity and temperature fields for various pertinent parameters are analyzed through plots with the help of MATHCAD software. The limiting cases are also provided to validate the present work.

2. Mathematical Formulation

Consider the unsteady free convection flow of incompressible Jeffrey hybrid nanofluid past an infinite vertical plate with constant temperature. The vertical plate serves as the x −axis and y −axis is chosen to be normal to it. This problem is modelled under the following assumptions [31,54-56]:

i. The fluid is assumed electrically conducting under influence of uniform transverse magnetic field of strength B_0 applied parallel to y −axis as shown in Figure 1.
ii. The low magnetic Reynolds number is taken, so that the effect of induced magnetic field can be neglected.
iii. It is also assumed that the external electric field is negligible due to the fact that zero applied and polarization voltage.
iv. Initially, at time t≤0, the plate and the fluid are at rest to a constant free stream temperature, T_∞.
v. At time $t > 0$ the temperature of the plate is raised or lowered to a constant temperature, T_w.
vi. The hybrid nanofluid flow phenomena are described using the Jeffrey fluid model. Additionally, the effects of heat absorption and thermal radiation are accounted in the energy equation.
vii. The nanoparticles are restricted to spherical shape and uniform size.
viii. Both nanoparticles and base fluid are considered in a stable condition with the same velocity flow.

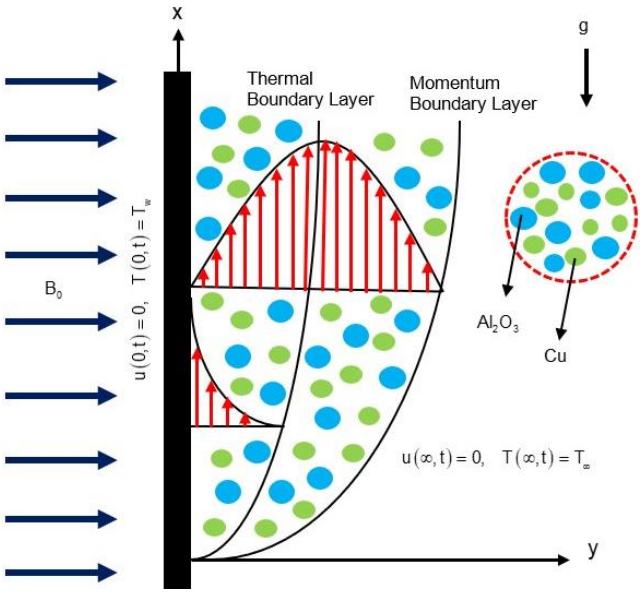

Fig. 1. Schematic diagram of Jeffrey hybrid nanofluid past an infinite vertical plate

Based on the above proposed assumptions and using the Boussinesq approximation, the governing equations of momentum and energy equations for unsteady free convection flow of hybrid nano-Jeffrey fluid adherence to Tiwari and Das Model past an infinite vertical plate with the impact of thermal radiation and heat absorption can be expressed as [57-62]:

$$\rho_{hnf}\frac{\partial u}{\partial t} = \frac{\mu_{hnf}}{1+\lambda_1}\left(1+\lambda_2\frac{\partial}{\partial t}\right)\frac{\partial^2}{\partial y^2} - \sigma B_0^2 u + g(\rho\beta_T)_{hnf}(T-T_\infty), \quad (1)$$

$$\left(\rho C_p\right)_{hnf}\frac{\partial T}{\partial t} = k_{hnf}\frac{\partial^2 T}{\partial y^2} - \frac{\partial q_r}{\partial y} - Q_0(T - T_\infty). \tag{2}$$

Provided that no-slip condition exists between the fluid and the plate. The appropriate initial and boundary conditions have been chosen as follows [59]:

$$u(y,0) = 0; \quad T(y,0) = T_\infty; \quad y \geq 0. \tag{3}$$

$$u(0,t) = 0; \quad T(0,t) = T_w; \quad t > 0, \tag{4}$$

$$u(\infty,t) = 0; \quad T(\infty,t) = T_\infty. \tag{5}$$

Here, ρ is the density, u is the velocity component in the x −direction, μ is the dynamic viscosity, λ_1 is the ratio of relaxation time and retardation time, λ_2 is the retardation time, σ is the electrical conductivity, g is the acceleration due to gravity, β_T is the volumetric coefficient of thermal expansion, T is the temperature, C_p is the specific heat at constant temperature, k is the thermal conductivity, q_r is the radiative heat flux, Q_0 is the heat absorption coefficient, and the subscript hnf, ∞ and w refer to hybrid nanofluid, free stream condition and condition at the surface, respectively.

Mathematically, the correlation of thermophysical properties for hybrid nanofluid are given by [62,63]:

$$\rho_{hnf} = \varphi_1\rho_1 + \varphi_2\rho_2 + \left(1 - \varphi_{hnf}\right)\rho_f, \text{ where } \varphi_{hnf} = \varphi_1 + \varphi_2. \tag{6}$$

$$\mu_{hnf} = \frac{\mu_f}{(1-\varphi_1-\varphi_2)^{2.5}}, \tag{7}$$

$$(\rho\beta_T)_{hnf} = \varphi_1(\rho\beta_T)_1 + \varphi_2(\rho\beta_T)_2 + \left(1 - \varphi_{hnf}\right)(\rho\beta_T)_f, \tag{8}$$

$$\left(\rho C_p\right)_{hnf} = \varphi_1\left(\rho C_p\right)_1 + \varphi_2\left(\rho C_p\right)_2 + \left(1 - \varphi_{hnf}\right)\left(\rho C_p\right)_f, \tag{9}$$

$$\frac{k_{hnf}}{k_f} = \frac{(k_{hp}+2k_f)-2\varphi_{hnf}(k_f-k_{hp})}{(k_{hp}+2k_f)+\varphi_{hnf}(k_f-k_{hp})}, \text{ where } k_{hp} = \frac{\varphi_1 k_1+\varphi_2 k_2}{\varphi_1+\varphi_2}. \tag{10}$$

Here, the subscripts $f, 1$ and 2 stand for the base fluid, Alumina, (Al_2O_3) and Copper, (Cu) nanoparticles, respectively. The thermophysical features of base fluids and nanoparticles are demonstrated in Table 1.

Table 1
The thermophysical features of base fluids and nanoparticles [62,64,65]

Physical properties	Base fluid			Nanoparticles	
	Ethylene Glycol	Kerosene	Water	Al_2O_3	Cu
$\boldsymbol{\rho}\ (\boldsymbol{kg/m^3})$	1115	780	997.1	3970	8933
$\boldsymbol{C_p}\ (\boldsymbol{J/kgK})$	2386	2090	4179	765	385
$\boldsymbol{k}\ (\boldsymbol{W/mK})$	0.2499	0.149	0.613	40	400
$\boldsymbol{\beta}\ (\boldsymbol{K^{-1}})$	3.41×10^{-3}	9.9×10^{-4}	21×10^{-5}	0.85×10^{-5}	01.67×10^{-5}
$\boldsymbol{Pr}$	203	21	6.2	-	-

The radiation heat flux, q_r under Rosseland approximation can be defined as [66-68]

$$q_r = -\frac{4\sigma^*}{3k_1}\frac{\partial T^4}{\partial y}, \tag{11}$$

where σ^* and k_1 denote the Stefan-Boltzmann constant and the coefficient of Rosseland absorption respectively. Since, the temperature differences within the flow are assumed to be very small, then using Taylor series expansion, T^4 about T_∞ can be expressed as

$$T^4 \cong T_\infty^4 + \frac{4T_\infty^3}{1!}(T - T_\infty) + \frac{12T_\infty^2}{2!}(T - T_\infty)^2 + \cdots \tag{12}$$

Hence, by emitting higher order, Eq. (12) takes the form of

$$T^4 \cong T_\infty^4 + 4T_\infty^3(T - T_\infty) = T_\infty^4 + 4T_\infty^3 T - 4T_\infty^4 = 4T_\infty^3 T - 3T_\infty^4. \tag{13}$$

Upon substituting Eq. (11) and Eq. (13) in Eq. (2), yields

$$\frac{\partial T}{\partial t} = \frac{k_f}{(\rho C_p)_{hnf}}\left(\frac{k_{hnf}}{k_f} + \frac{16}{3}\frac{\sigma^* T_\infty^3}{k_f k_1}\right)\frac{\partial^2 T}{\partial y^2} - \frac{1}{(\rho C_p)_{hnf}}Q_0(T - T_\infty). \tag{14}$$

Introducing the following dimensionless variables [59,60]:

$$u^* = \frac{u}{U_0}, \quad t^* = \frac{tU_0^2}{\upsilon_f}, \quad y^* = \frac{yU_0}{\upsilon_f}, \quad \theta = \frac{T - T_\infty}{T_w - T_\infty}, \tag{15}$$

into Eq. (1) to Eq. (5) and make use of relations in Eq. (6) to Eq. (10), leads to the expressions of non-dimensional partial differential equations (for simplicity, omit the star notations)

$$\xi_0\frac{\partial u}{\partial t} = \left(\frac{\xi_1}{1+\lambda_1}\right)\left(1 + \lambda\frac{\partial}{\partial t}\right)\frac{\partial^2 u}{\partial y^2} - (Ha)u + \xi_2(Gr)\theta, \tag{16}$$

$$\eta_1\frac{\partial \theta}{\partial t} = \frac{\eta_2}{Pr}\frac{\partial^2 \theta}{\partial y^2} - Q\theta. \tag{17}$$

Subject to initial and boundary conditions:

$$u(y,0) = 0; \qquad \theta(y,0) = 0; \qquad y \geq 0, \tag{18}$$

$$u(0,t) = 0; \qquad \theta(0,t) = 1; \qquad t > 0, \tag{19}$$

$$u(\infty,t) = 0; \qquad \theta(\infty,t) = 0; \qquad t > 0. \tag{20}$$

In which, λ is the dimensionless Jeffrey parameter, Ha is the Hartmann number, Gr is the Grashof number, Pr is the Prandtl number and Q is the heat absorption parameter. These parameters can be defined as follows:

$$\lambda = \frac{\lambda_2 U_0^2}{\nu_f}, \quad Ha = \frac{\sigma B_0^2 \nu_f}{\rho_f U_0^2}, \quad Gr = \frac{g(\beta_T \nu)_f (T_w - T_\infty)}{U_0^3}, \quad Pr = \frac{\nu_f}{\alpha_f}, \quad Q = \frac{Q_0}{U_0}\left(\frac{\nu}{\rho C_p}\right)_f,$$

where

$$\alpha_f = \frac{k_f}{(\rho C_p)_f}. \tag{21}$$

The arbitrary constants are given by

$$\xi_0 = \left(\frac{\varphi_1\rho_1+\varphi_2\rho_2}{\rho_f}\right) + (1-\varphi_1-\varphi_2), \tag{22}$$

$$\xi_1 = \frac{1}{(1-\varphi_1-\varphi_2)^{2.5}}, \tag{23}$$

$$\xi_2 = \frac{\varphi_1(\rho\beta_T)_1+\varphi_2(\rho\beta_T)_2}{(\rho\beta_T)_f} + (1-\varphi_1-\varphi_2), \tag{24}$$

$$\eta_1 = \frac{\varphi_1(\rho C_p)_1+\varphi_2(\rho C_p)_2}{(\rho C_p)_f} + (1-\varphi_1-\varphi_2), \tag{25}$$

$$\eta_2 = \frac{k_{nnf}}{k_f} + Rd. \tag{26}$$

Here, Rd is the radiation parameter which can be written as

$$Rd = \frac{16}{3}\frac{\sigma^* T_\infty^3}{k_f k_1}. \tag{27}$$

3. Solution of the Problem

There are two methods to solve the above partial differential equations, namely analytical method, and numerical approach. However, in this study, an analytical method is chosen to solve the present problem with the help of Laplace transform technique. Thus, applying the Laplace transform to Eq. (16) to Eq. (20) leads to the following transformed system in (y, q) −plane:

$$\xi_0[q\bar{u}(y,q)-\bar{u}(y,0)] = \left(\frac{\xi_1}{1+\lambda_1}\right)\frac{d^2\bar{u}(y,q)}{dy^2} + \left(\frac{\lambda\xi_1}{1+\lambda_1}\right)\frac{d^2}{dy^2}[q\bar{u}(y,q)-\bar{u}(y,0)] - (Ha)\bar{u}(y,q) + \xi_2(Gr)\bar{\theta}(y,q), \tag{28}$$

$$\eta_1[q\bar{\theta}(y,q)-\bar{\theta}(y,0)] = \frac{\eta_2}{Pr}\frac{d^2\bar{\theta}(y,q)}{dy^2} - Q\bar{\theta}(y,q), \tag{29}$$

together with the transform initial and boundary conditions below:

$$\bar{u}(y,0) = 0; \qquad \bar{\theta}(y,0) = 0, \tag{30}$$

$$\bar{u}(0,q) = 0; \qquad \bar{u}(\infty,q) = 0, \tag{31}$$

$$\bar{\theta}(0,q) = \frac{1}{q}; \qquad \bar{\theta}(\infty,q) = 0. \tag{32}$$

Here, $\bar{u}(y,q)$ and $\bar{\theta}(y,q)$ denotes the Laplace transforms of $u(y,t)$ and $\theta(y,t)$. Now, using Eq. (30) into Eq. (28) and Eq. (29), yields to

$$\xi_0 q\bar{u}(y,q) = \left(\frac{\xi_1}{1+\lambda_1}\right)\frac{d^2\bar{u}(y,q)}{dy^2} + \left(\frac{\lambda\xi_1}{1+\lambda_1}q\right)\frac{d^2\bar{u}(y,q)}{dy^2} - (Ha)\bar{u}(y,q) + \xi_2(Gr)\bar{\theta}(y,q), \tag{33}$$

$$\frac{d^2\theta(y,q)}{dy^2} - \left[\frac{Pr}{\eta_2}(Q+\eta_2 q)\right]\bar{\theta}(y,q) = 0. \tag{34}$$

Since there exists the term of energy equation in Eq. (33), therefore, it is much simpler to solve the energy equation first rather than the momentum equation. Invoking Eq. (32) into Eq. (34), then

$$\bar{\theta}(y,q) = \frac{1}{q}e^{-y\sqrt{\frac{\eta_1 Pr}{\eta_2}}\sqrt{q+\frac{Q}{\eta_1}}}. \tag{35}$$

the inverse Laplace transform of Eq. (35), gives the required temperature distribution as

$$\theta(y,t) = \frac{1}{2}e^{y\sqrt{\frac{QPr}{\eta_2}}}.erfc\left(\frac{y}{2}\sqrt{\frac{\eta_1 Pr}{\eta_2 t}} + \sqrt{\frac{Qt}{\eta_1}}\right) + \frac{1}{2}e^{-y\sqrt{\frac{QPr}{\eta_2}}}.erfc\left(\frac{y}{2}\sqrt{\frac{\eta_1 Pr}{\eta_2 t}} - \sqrt{\frac{Qt}{\eta_1}}\right). \tag{36}$$

In Eq. (36), $erfc(\cdot)$ is the complementary error function which can defined as

$$erf(x) = 1 - erfc(x); \qquad erfc(x) = 2\int_x^\infty \frac{1}{\sqrt{x}}e^{-u^2}du. \tag{37}$$

Plugging Eq. (35) into Eq. (33) and make use of Eq. (31) gives

$$\bar{u}(y,q) = \left(\frac{a_1\eta_2}{a_2}\right)[\bar{u}_1(y,q) - \bar{u}_2(y,q)], \tag{38}$$

where,

$$\bar{u}_1(y,q) = \left(\frac{1}{q}\right)\left(\frac{1}{(q+b_0)^2 - b_1}\right)e^{-y\sqrt{a_0\left(\frac{Ha+\xi_0 q}{1+\lambda q}\right)}}, \tag{39}$$

$$\bar{u}_2(y,q) = \left(\frac{1}{q}\right)\left(\frac{1}{(q+b_0)^2 - b_1}\right)e^{-y\sqrt{\frac{\eta_1 Pr}{\eta_2}}\sqrt{q+\frac{Q}{\eta_1}}}. \tag{40}$$

Here arbitrary constants are given by:

$$a_0 = \frac{1+\lambda_1}{\xi_1}, \qquad a_1 = \frac{\xi_2 Gr}{\xi_1}(1+\lambda_1), \qquad a_2 = \lambda\eta_1 Pr, \qquad b_0 = \frac{a_3}{2a_2}, \qquad b_1 = \frac{(a_3)^2 - 4a_2a_4}{4(a_2)^2}. \tag{41}$$

In which,

$$a_3 = (\eta_1 + \lambda Q)Pr - a_0\eta_2\xi_0, \qquad a_4 = QPr - a_0\eta_2 Ha. \tag{42}$$

In order to determine the inverse Laplace transform of Eq. (39), we set up it in the form of

$$\bar{u}_1(y,q) = \bar{F}_1(q).\bar{F}_2(y,q). \tag{43}$$

In which,

$$\bar{F}_1(q) = \frac{1}{(q+b_0)^2 - b_1}, \tag{44}$$

$$\bar{F}_2(y,q) = \frac{1}{q} e^{-y\sqrt{a_0\left(\frac{Ha+\xi_0 q}{1+\lambda q}\right)}}. \tag{45}$$

Taking the inverse Laplace transform of Eq. (44) implies

$$F_1(t) = \frac{1}{\sqrt{b_1}} e^{-b_0 t} sinh\left(\sqrt{b_1} t\right). \tag{46}$$

Now, split Eq. (45) into

$$\bar{F}_{21}(q) = \frac{1}{q}, \tag{47}$$

$$\bar{F}_{22}(y,q) = e^{-y\sqrt{\frac{a_0 Ha + a_0 \xi_0 q}{1+\lambda q}}}. \tag{48}$$

The inversion Laplace transform of Eq. (47) is given by

$$F_{21}(t) = 1. \tag{49}$$

Let Eq. (48) as

$$\bar{F}_{22}(y,q) = e^{-y\sqrt{w(q)}}, \text{ where } w(q) = \frac{a_0 Ha + (a_0 \xi_0) q}{1+\lambda q}. \tag{50}$$

Following Nazar *et al.,* [69], the inverse Laplace transform of Eq. (50) can be determined using the inversion formula of compound function such that

$$F_{22}(y,t) = \int_0^\infty f(y,u) g(u,t) du, \tag{51}$$

where

$$f(y,u) = \frac{y}{2u\sqrt{\pi u}} e^{-\left(\frac{y^2}{4u}\right)}, \tag{52}$$

$$g(u,t) = e^{-ud_0}\delta(t) + \sqrt{\frac{ud_1}{t}} e^{-ud_0 - \frac{t}{\lambda}} I_1\left(2\sqrt{ud_1 t}\right). \tag{53}$$

Here, $\delta(\cdot)$ is Dirac delta function, $I_1(\cdot)$ is the modified Bessel function of the first kind of order one and the arbitrary constants are given as follows

$$d_0 = \frac{a_0 \xi_0}{\lambda}, \qquad d_1 = \frac{a_0 \xi_0}{\lambda^2} - \frac{a_0 Ha}{\lambda}. \tag{54}$$

Hence, make use of Eq. (52) and Eq. (53) into Eq. (51) yielding the following simplified form:

$$F_{22}(y,t) = \delta(t)e^{-y\sqrt{d_0}} + \int_0^\infty \frac{y}{2u}\sqrt{\frac{d_1}{\pi t}}\, e^{-\frac{y^2}{4u}-ud_0-\frac{t}{\lambda}} I_1\left(2\sqrt{ud_1t}\right)du. \tag{55}$$

In order to determine the function $F_2(y,t)$ in Eq. (45), we need to use the convolution theorem as being given by:

$$F_2(y,t) = (F_{21} * F_{22})(t) = \int_0^t F_{21}(t-s).F_{22}(y,s)ds. \tag{56}$$

Incorporating Eq. (49) and Eq. (55) into Eq. (56), and after further simplification, the function $F_2(y,t)$ takes the following form:

$$F_2(y,t) = e^{-y\sqrt{d_0}} + \int_0^t \int_0^\infty \frac{y}{2u}\sqrt{\frac{d_1}{\pi s}}\, e^{-\frac{y^2}{4u}-ud_0-\frac{s}{\lambda}} I_1\left(2\sqrt{ud_1s}\right)duds. \tag{57}$$

Since, Eq. (43) involves multiplication of two functions of $\bar{F}_1(q)$ and $\bar{F}_2(y,q)$, again the convolution theorem is utilized. Hence it can be written as

$$\begin{aligned} u_1(y,t) = (F_1 * F_2)(t) &= \int_0^t F_1(t-p).F_2(y,p)dp \\ &= \int_0^t \frac{1}{\sqrt{b_1}} e^{-b_0(t-p)-y\sqrt{d_0}} sinh\left(\sqrt{b_1(t-p)}\right)dp \\ &\quad + \int_0^t \int_0^p \int_0^\infty \frac{y}{2u}\sqrt{\frac{d_1}{\pi b_1 s}}\, e^{-b_0(t-p)-\frac{y^2}{4u}-ud_0-\frac{s}{\lambda}} sinh\left(\sqrt{b_1}(t-p)\right) \times I_1\left(2\sqrt{ud_1s}\right)dudsdp. \end{aligned} \tag{58}$$

Furthermore, to evaluate the function $\bar{u}_2(y,q)$, we split Eq. (40) into

$$\bar{u}_2(y,q) = \bar{F}_1(q).\bar{F}_3(y,q), \tag{59}$$

where $\bar{F}_1(q)$ as in Eq. (44) and

$$\bar{F}_3(y,q) = \frac{1}{q} e^{-y\sqrt{\frac{\eta_1 Pr}{\eta_2}}\sqrt{q+\frac{Q}{\eta_1}}}. \tag{60}$$

Following Hetnarski [70], The inversion Laplace transform of Eq. (60) can be obtained as follows:

$$F_3(y,t) = \frac{1}{2} e^{y\sqrt{\frac{QPr}{\eta_2}}} erfc\left(\frac{y}{2}\sqrt{\frac{\eta_1 Pr}{\eta_2 t}} + \sqrt{\frac{Qt}{\eta_1}}\right) + \frac{1}{2} e^{-y\sqrt{\frac{QPr}{\eta_2}}} erfc\left(\frac{y}{2}\sqrt{\frac{\eta_1 Pr}{\eta_2 t}} - \sqrt{\frac{Qt}{\eta_1}}\right). \tag{61}$$

Since, Eq. (40) involves multiplication of two functions of $\bar{F}_1(q)$ and $\bar{F}_3(y,q)$, again the convolution theorem

$$u_2(y,t) = (F_1 * F_3)(t) = \int_0^t F_1(t-s).F_3(y,s)ds \tag{62}$$

is used. Then,

$$u_2(y,t) = \int_0^t \frac{1}{2\sqrt{b_1}} e^{-b_0(t-s)+y\sqrt{\frac{QPr}{\eta_2}}} sinh\left[\sqrt{b_1}(t-s)\right] erfc\left(\frac{y}{2}\sqrt{\frac{\eta_1 Pr}{\eta_2 s}} + \sqrt{\frac{Qs}{\eta_1}}\right) ds +$$
$$\int_0^t \frac{1}{2\sqrt{b_1}} e^{-b_0(t-s)-y\sqrt{\frac{QPr}{\eta_2}}} sinh\left[\sqrt{b_1}(t-s)\right] erfc\left(\frac{y}{2}\sqrt{\frac{\eta_1 Pr}{\eta_2 s}} - \sqrt{\frac{Qs}{\eta_1}}\right). \quad (63)$$

Thus, the solution of velocity profile in Eq. (38) can be written as

$$u(y,t) = \left(\frac{a_1\eta_2}{a_2}\right)[u_1(y,t) - u_2(y,t)]. \quad (64)$$

In which the functions of $u_1(y,t)$ and $u_2(y,t)$ are given by Eq. (58) and Eq. (63) respectively.

4. Nusselt Number and Skin Friction

The rate of heat transfer or Nusselt number, Nu and the coefficient of skin friction, τ are defined as

$$Nu = -\frac{\partial\theta}{\partial y}\Big|_{y=0}, \quad (65)$$

$$\tau = \frac{1}{1+\lambda_1}\left(1 + \lambda\frac{\partial}{\partial t}\right)\frac{\partial u}{\partial y}\Big|_{y=0}. \quad (66)$$

Plugging Eq. (36) into Eq. (65) and Eq. (64) into Eq. (66), therefore

$$Nu = -\frac{1}{2}\sqrt{\frac{QPr}{\eta_2}} erfc\left(\sqrt{\frac{Qt}{\eta_1}}\right) + \sqrt{\frac{Pr\eta_1}{\pi\eta_2}} e^{-\sqrt{\frac{Qt}{\eta_1}}} + \frac{1}{2}\sqrt{\frac{QPr}{\eta_2}} erfc\left(-\sqrt{\frac{Qt}{\eta_1}}\right), \quad (67)$$

$$\tau = \frac{1}{1+\lambda_1}\left(\frac{a_1\eta_2}{a_2}\right)[\Psi_1(t) + \Psi_2(t) - \Psi_3(t) + \Psi_4(t)]$$
$$+\frac{\lambda}{1+\lambda_1}\left(\frac{a_1\eta_2}{a_2}\right)[\Phi_1(t) + \Phi_2(t) - \Phi_3(t) + \Phi_4(t)] \quad (68)$$

In which the components of $\Psi_i(i = 1,2,3,4)$ and $\Phi_j(j = 1,2,3,4)$ are given by

$$\Psi_1(t) = -\sqrt{\frac{d_0}{b_1}}\left[\frac{\sqrt{b_1}e^{-b_0 t}cosh(\sqrt{b_1}t) - \sqrt{b_1} + b_0 e^{-b_0 t}sinh(\sqrt{b_1}t)}{b_1 - b_0^2}\right], \quad (69)$$

$$\Psi_2(t) = \int_0^t \int_0^p \int_0^\infty \frac{1}{2u}\sqrt{\frac{d_1}{\pi b_1 s}} e^{b_0(p-t)-ud_0-\frac{s}{\lambda}} \times sinh\left[\sqrt{b_1}(t-p)\right] I_1\left(2\sqrt{ud_1 s}\right) du ds dp, \quad (70)$$

$$\Psi_3(t) = \int_0^t \frac{1}{2\sqrt{b_1}} e^{b_0(s-t)} sinh\left[\sqrt{b_1}(t-s)\right] \times \left[\sqrt{\frac{QPr}{\eta_2}} erfc\left(\sqrt{\frac{Qs}{\eta_2}}\right) - \frac{1}{\sqrt{\pi}} e^{\frac{Qs}{\eta_2}}\sqrt{\frac{\eta_1 Pr}{s\eta_2}}\right] ds, \quad (71)$$

$$\Psi_4(t) = \int_0^t \frac{1}{2}\sqrt{\frac{Pr}{\eta_2 b_1}} e^{b_0(s-t)} sinh\left[\sqrt{b_1(t-s)}\right] \times \left[\sqrt{Q} erfc\left(-\sqrt{\frac{Qs}{\eta_2}}\right) + \sqrt{\frac{\eta_1}{s\pi}} e^{-\frac{Qs}{\eta_2}}\right] ds, \quad (72)$$

and

$$\Phi_1(t) = \sqrt{\frac{d_0}{b_1}}\left[\frac{b_0^2 e^{-b_0 t}sinh(\sqrt{b_1}t) - b_1 e^{-b_0 t}sinh(\sqrt{b_1}t)}{b_1 - b_0^2}\right], \tag{73}$$

$$\Phi_2(t) = \int_0^t \int_0^p \int_0^\infty \left[b_0 e^{-b_0 t}sinh\left[\sqrt{b_1}(p-t)\right] + \sqrt{b_1}e^{-b_0 t}cosh\left[\sqrt{b_1}(p-t)\right]\right] \times \frac{1}{2u}\sqrt{\frac{d_1}{b_1 \pi s}}e^{b_0 p - ud_0 - \frac{s}{\lambda}} \times I_1\left(2\sqrt{ud_1 s}\right)dudsdp, \tag{74}$$

$$\Phi_3(t) = \int_0^t \frac{b_0 e^{b_0(s-t)}}{2}\sqrt{\frac{Pr}{b_1 \eta_2}}\left[\sqrt{Q}erfc\left(\sqrt{\frac{Qs}{\eta_2}}\right) - \sqrt{\frac{\eta_1}{\pi}}e^{\frac{Qs}{\eta_2}}\right] \times \left[sinh\left[\sqrt{b_1(s-t)}\right] + \sqrt{b_1}cosh\left[\sqrt{b_1}(s-t)\right]\right]ds, \tag{75}$$

$$\Phi_4(t) = \int_0^t \frac{1}{2}\sqrt{\frac{Pr}{b_1 \eta_2}}\left[\sqrt{Q}erfc\left(-\sqrt{\frac{Qs}{\eta_2}}\right) + \sqrt{\frac{Pr\eta_1}{s\pi}}e^{-\frac{Qs}{\eta_2}}\right] \times \left[b_0 e^{b_0(s-t)}sinh\left[\sqrt{b_1}(s-t)\right] + \sqrt{b_1}e^{b_0(s-t)}cosh\left[\sqrt{b_1(s-t)}\right]\right]ds. \tag{76}$$

5. Special Cases

In this section, closed-form solutions for two special cases are provided by taking suitable parameters equal to zero.

5.1 Case 1: $\lambda_1 = 0$

Surprisingly, by taking $\lambda_1 = 0$, the obtained velocity profile in Eq. (64) can be reduced to the problem of second grade hybrid nanofluid with heat absorption and radiation effects. This implies:

$$u(y,t) = \frac{\xi_2 \eta_2 Gr}{\xi_1 \eta_1 \lambda Pr}\left[\frac{1}{\sqrt{b_{11}}}u_{11}(y,t) + \frac{1}{2}\sqrt{\frac{d_{11}}{\pi b_{11}}}u_{12}(y,t) - \frac{1}{2\sqrt{b_{11}}}u_{13}(y,t) - \frac{1}{2\sqrt{b_{11}}}u_{14}(y,t)\right], \tag{77}$$

where

$$u_{11}(y,t) = \int_0^t e^{b_{01}(p-t) - y\sqrt{d_{01}}}sinh\left(\sqrt{b_{11}(t-p)}\right)dp, \tag{78}$$

$$u_{12}(y,t) = \int_0^t \int_0^p \int_0^\infty \frac{y}{u\sqrt{s}}e^{b_{01}(p-t) - \frac{y^2}{4u} - ud_{01} - \frac{s}{\lambda}}sinh\left(\sqrt{b_{11}}(t-p)\right) \times I_1\left(2\sqrt{ud_{11}s}\right)dudsdp\,, \tag{79}$$

$$u_{13}(y,t) = \int_0^t e^{b_{01}(s-t) + y\sqrt{\frac{QPr}{\eta_2}}}sinh\left[\sqrt{b_{11}}(t-s)\right]erfc\left(\frac{y}{2}\sqrt{\frac{\eta_1 Pr}{\eta_2}} + \sqrt{\frac{Qs}{\eta_1}}\right)ds, \tag{80}$$

$$u_{14}(y,t) = \int_0^t e^{b_{01}(s-t) - y\sqrt{\frac{QPr}{\eta_2}}}sinh\left(\sqrt{b_{11}}(t-s)\right)erfc\left(\frac{y}{2}\sqrt{\frac{\eta_1 Pr}{\eta_2 s}} - \sqrt{\frac{Qs}{\eta_1}}\right)ds. \tag{81}$$

In which the arbitrary parameters are given by

$$a_{31} = \eta_1 Pr + \lambda QPr - \frac{\eta_2 \xi_0}{\xi 1}, \qquad a_{41} = QPr - \frac{\eta_2 Ha}{\xi_1},$$
$$b_{01} = \frac{a_{31}}{2a_2}, \qquad b_{11} = \frac{(a_{31})^2 - 4a_2 a_{41}}{4(a_2)^2},$$
$$d_{01} = \frac{\xi_0}{\lambda \xi_1}, \qquad d_{11} = \frac{1}{\lambda \xi_1}\left(\frac{\xi_0}{\lambda} - Ha\right). \tag{82}$$

5.2 Case 2: $\varphi_1 = \varphi_2 = 0$

In addition, substituting $\varphi_1 = \varphi_2 = 0$, into Eq. (64) leads to the following expression:

$$u(y,t) = \frac{(1+\lambda_1)(1+Rd)Gr}{\lambda Pr}\left[\frac{1}{\sqrt{b_{12}}}u_{21}(y,t) + \frac{1}{2}\sqrt{\frac{d_{12}}{\pi b_{12}}}u_{22}(y,t) - \frac{1}{2\sqrt{b_{12}}}u_{23}(y,t) - \frac{1}{2\sqrt{b_{12}}}u_{24}(y,t)\right]. \tag{83}$$

Here,

$$u_{21}(y,t) = \int_0^t e^{b_{02}(p-t) - y\sqrt{\frac{1+\lambda_1}{\lambda}}} sinh\left(\sqrt{b_{12}(t-p)}\right) dp, \tag{84}$$

$$u_{12}(y,t) = \int_0^t \int_0^p \int_0^\infty \frac{y}{u\sqrt{s}} e^{b_{02}(p-t) - \frac{y^2}{4u} - u\left(\frac{1+\lambda_1}{\lambda}\right) - \frac{s}{\lambda}} sinh\left(\sqrt{b_{12}}(t-p)\right) \times I_1\left(2\sqrt{ud_{12}s}\right) du ds dp, \tag{85}$$

$$u_{23}(y,t) = \int_0^t e^{b_{02}(s-t) + y\sqrt{\frac{QPr}{1+Rd}}} sinh\left[\sqrt{b_{12}}(t-s)\right] \times erfc\left(\frac{y}{2}\sqrt{\frac{Pr}{1+Rd}} + \sqrt{Qs}\right) ds, \tag{86}$$

$$u_{24}(y,t) = \int_0^t e^{b_{02}(s-t) - y\sqrt{\frac{QPr}{1+Rd}}} sinh\left(\sqrt{b_{12}}(t-s)\right) \times erfc\left(\frac{y}{2}\sqrt{\frac{Pr}{(1+Rd)s}} - \sqrt{Qs}\right) ds, \tag{87}$$

and

$$b_{02} = \frac{Pr(1+\lambda Q) + (1+\lambda_1)(1+Rd)}{2\lambda Pr},$$
$$b_{12} = \left[\frac{Pr(1+\lambda Q) + (1+\lambda_1)(1+Rd)}{2\lambda Pr}\right]^2 - \frac{1}{\lambda}[Q + (1+Rd)Ha],$$
$$d_{12} = \frac{(1+\lambda_1)}{\lambda}\left(\frac{1}{\lambda} - Ha\right). \tag{88}$$

It corresponds to the general unsteady MHD free convection flow of Jeffrey fluid with the effects of radiation and heat absorption. However, by taking $Rd = 0$ and $Q = 0$ into Eq. (36) and $Rd = 0$, $Q = 0$ and $Ha = 0$ into Eq. (83), leads to

$$\theta(y,t) = erfc\left(\frac{y}{2}\sqrt{\frac{Pr}{t}}\right) \tag{89}$$

$$u(y,t) = \frac{2Gr(1+\lambda_1)}{Pr+1+\lambda_1}\int_0^t e^{\frac{Pr+1+\lambda_1}{2\lambda Pr}(p-t)-y\sqrt{\frac{1+\lambda_1}{\lambda}}} sinh\left[\left(\frac{Pr+1+\lambda_1}{2\lambda Pr}\right)(t-p)\right]dp + \frac{Gr(1+\lambda_1)}{\lambda(Pr+1+\lambda_1)}\sqrt{\frac{1+\lambda_1}{\pi}}\int_0^t\int_0^p\int_0^\infty \frac{y}{u\sqrt{s}} e^{\frac{Pr+1+\lambda_1}{2\lambda Pr}(p-t)-\frac{y^2}{4u}-u\left(\frac{1+\lambda_1}{\lambda}\right)-\frac{s}{\lambda}} \times sinh\left[\left(\frac{Pr+1+\lambda_1}{2\lambda Pr}\right)(t-p)\right] I_1\left(\frac{2}{\lambda}\sqrt{u(1+\lambda_1)s}\right) dudsdp - \frac{Gr(1+\lambda_1)}{Pr+1+\lambda_1}\int_0^t e^{\left(\frac{Pr+1+\lambda_1}{2\lambda Pr}\right)(s-t)} sinh\left[\left(\frac{Pr+1+\lambda_1}{2\lambda Pr}\right)(t-s)\right] \times erfc\left(\frac{y}{2}\sqrt{Pr}\right)ds - \frac{Gr(1+\lambda_1)}{Pr+1+\lambda_1}\int_0^t e^{\left(\frac{Pr+1+\lambda_1}{2\lambda Pr}\right)(s-t)} sinh\left[\left(\frac{Pr+1+\lambda_1}{2\lambda Pr}\right)(t-s)\right] \times erfc\left(\frac{y}{2}\sqrt{\frac{Pr}{s}}\right)ds, \quad (90)$$

respectively, which is identical to the previous work obtained by Khan [59].

6. Results and Discussions

This section discussed several connected parameters such as radiation parameter Rd, heat absorption parameter Q, Hartmann number Ha, Grashof Number Gr, dimensionless material parameter λ, volume fraction of hybrid nanofluid φ_{hnf}, dimensionless time t and Prandtl number Pr on velocity and temperature distributions. The physical model is given in Figure 1. The results of temperature and velocity profiles in Eq. (36) and (64) are computed using MATHCAD software. Figure 2 illustrates the radiation impact on the hybrid nanofluid flow. As can be seen in the graph, velocity of the hybrid nanofluid increases when radiation parameter increases. This phenomenon is observed since the bond of nanofluid's particles are easily disrupted due to the increases of rate energy transmission when radiation parameter rises. Hence, it reduces the nanofluid's viscosity and enhance hybrid nanofluid flow. The variation of heat absorption influence velocity profile is presented in Figure 3. It is found that increases of heat absorption cause velocity profiles to decrease. The occurrence of heat absorption (heat sink) reduces the thermal energy of fluid which leads to increase the viscous force of fluid. Thus, the velocity of hybrid nanofluid is decelerated.

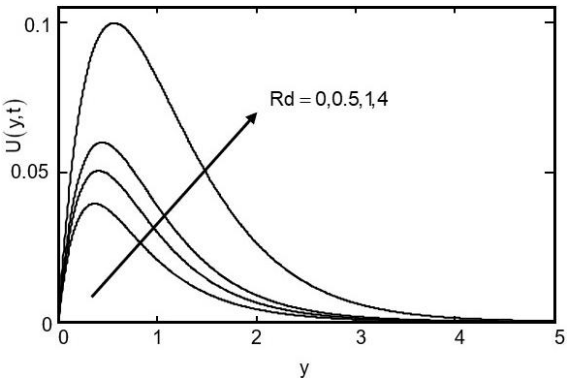

Fig. 2. Velocity profile for different value of Rd, when $\lambda_1 = 1$, $\lambda = 1$, $Ha = 2$, $Q = 2$, $Pr = 6.2$, $Gr = 1.5$, $t = 1$ and $\varphi_{hnf} = 0.04$

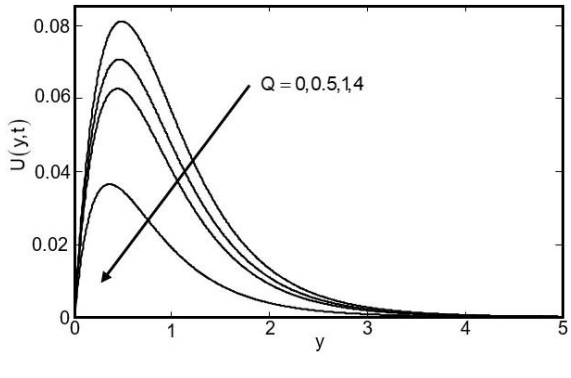

Fig. 3. Velocity profile for different value of Q, when $\lambda_1 = 1$, $\lambda = 1$, $Ha = 2$, $Rd = 0.5$, $Pr = 6.2$, $Gr = 1.5$, $t = 1$ and $\varphi_{hnf} = 0.04$

Figure 4 displays the effect of the MHD on the velocity profiles. It is shown that velocity profiles with the existence of the MHD effect, $Ha = 1,2,3$ are higher than velocity profile with no MHD effect, $Ha = 0$. Besides that, velocity profiles diminish with the increasing of MHD parameter. It is due to the drag force produced from the induced current retard the hybrid nanofluid flow when electrical conducting fluid flow across the external magnetic field. The Grashof number effect on the velocity profiles is depicted in Figure 5. Based on the graph observation, velocity distribution inclined with the increment of the Grashof number. It is because buoyancy force rises as temperature gradient

increases and causes reduction of viscous force acting on a fluid. Thus, it enhances the hybrid nanofluid flow.

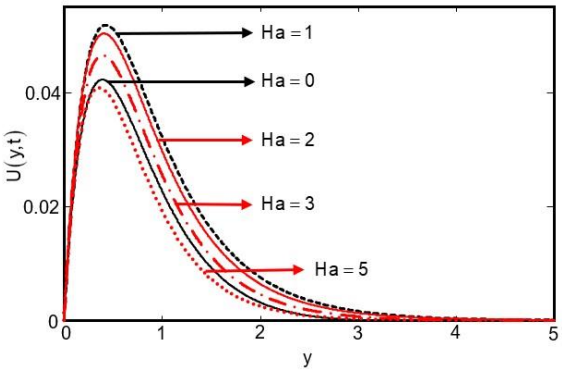

Fig. 4. Velocity profile for different value of Ha, when $\lambda_1 = 1,\ \lambda = 1,\ Q = 2,\ Rd = 0.5,\ Pr = 6.2, Gr = 1.5, t = 1$ and $\varphi_{hnf} = 0.04$

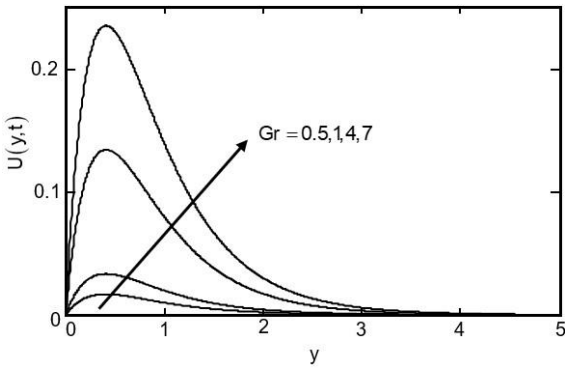

Fig. 5. Velocity profile for different value of Gr, when $\lambda_1 = 1,\ \lambda = 1,\ Q = 2,\ Rd = 0.5,\ Pr = 6.2, Ha = 2, t = 1$ and $\varphi_{hnf} = 0.04$

Figure 6 to 8 are represented the Jeffrey parameters impact on the velocity profiles. For both cases of increasing the relaxation to retardation time ratio, λ and $\lambda = \lambda_1$. As shown in Figure 6 and 7, the velocity profiles decrease at $y < 1.5$. However, velocity profiles increase at $y > 1.5$. Inversely as can be seen in Figure 8, the velocity field is an increasing function of retardation time, λ_1 at $y < 1.5$ while the velocity field is a decreasing function of λ_1 at $y > 1.5$. It is because λ and λ_1 are viscoelastic parameters that exhibit both elastic and viscous behavior which influence the fluid flow velocity.

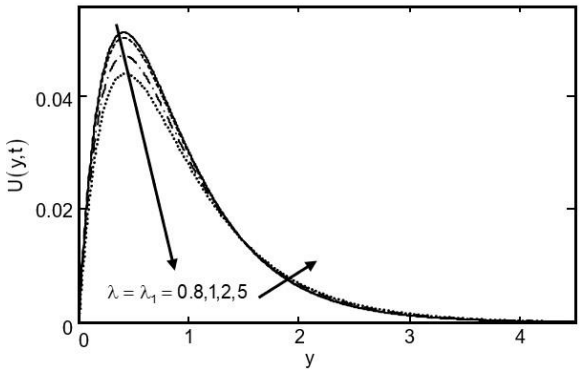

Fig. 6. Velocity profile for different value of λ and λ_1, when $Q = 2, Rd = 0.5, Pr = 6.2, Gr = 1.5, t = 1$ and $\varphi_{hnf} = 0.04$

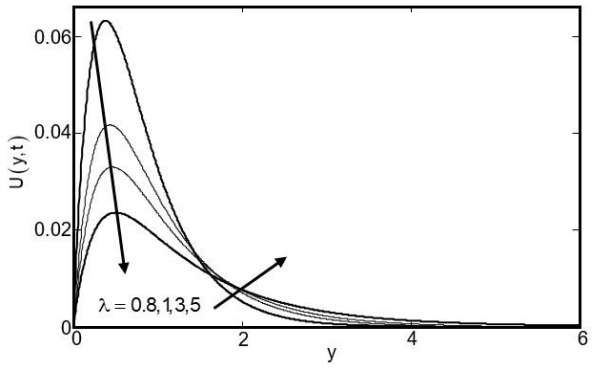

Fig. 7. Velocity profile for different value of λ, when $\lambda_1 = 1.5, Gr = 1.5, Q = 2, Rd = 0.5, Pr = 6.2, Ha = 2, t = 1$ and $\varphi_{hnf} = 0.04$

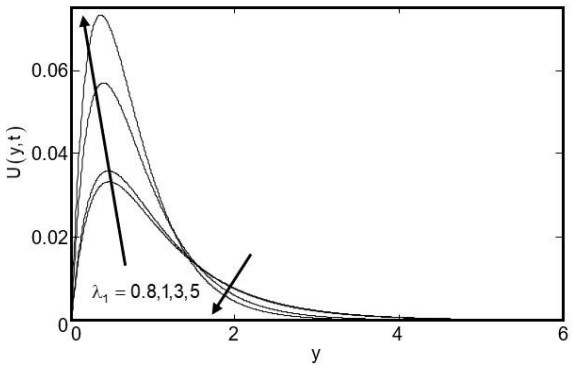

Fig. 8. Velocity profile for different value of λ_1, when $\lambda = 1.5, Gr = 1.5, Q = 2, Rd = 0.5, Pr = 6.2, Ha = 2, t = 1$ and $\varphi_{hnf} = 0.04$

Figure 9 demonstrates the effects of several base fluid types (water, kerosene, and ethylene glycols (EG)) on the velocity profiles. It is found that water has maximum velocity, followed by kerosene, and ethylene glycols. It indicates that water has the lowest viscosity when compared with other types of base fluid. The influence of the hybrid nanofluid in the regular Jeffrey fluid can be seen in Figure 10. It is found that by increasing the nanoparticle volume fraction of hybrid nanofluid, φ_{hnf} the velocity profiles fall. It is justified by rising φ_{hnf}, the hybrid nanofluid got denser and concentrated. Hence, thermal conductivity of hybrid nanofluid is dominated by the effective density of hybrid nanofluid, which causes the velocity profile to decline.

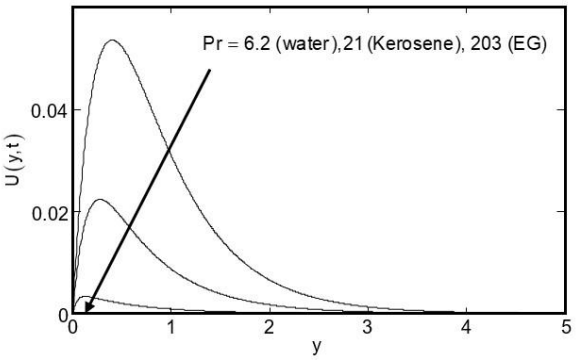

Fig. 9. Velocity profile for different value of Pr, when $\lambda_1 = \lambda = 1,\ Gr = 1.5,\ Q = 2,\ Rd = 0.5,\ Ha = 2, t = 1$ and $\varphi_{hnf} = 0.005$

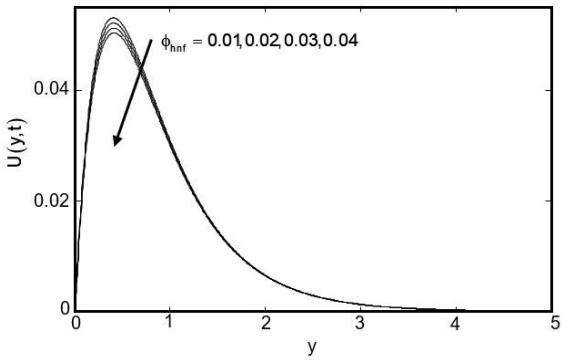

Fig. 10. Velocity profile for different value of φ_{hnf}, when $\lambda_1 = 1,\ \lambda = 1,\ Ha = 2,\ Q = 2,\ Pr = 6.2, Gr = 1.5, t = 1$ and $Rd = 0.5$

The comparison of velocity distribution between nanofluids and regular Jeffrey fluid can be seen in Figure 11. It is discovered that regular Jeffrey fluid has the highest amplitude, followed by nanofluids and then hybrid nanofluids. This indicates that the viscosity of the regular Jeffrey fluid is the lowest among other nanofluids. Hence, regular Jeffrey fluid is the fastest flow while the hybrid nanofluid is the slowest flow.

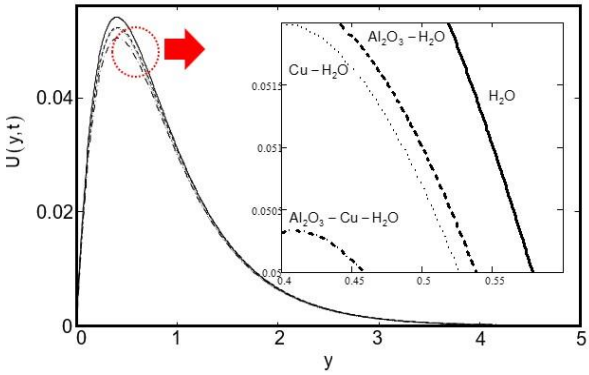

Fig. 11. Comparison of velocity profile for different nanofluids and regular Jeffrey fluid, when $\lambda_1 = 1$, $\lambda = 1$, $Ha = 2$, $Q = 2$, $Pr = 6.2$, $Gr = 1.5$, $t = 1$, $Rd = 0.5$ and $Pr = 6.2$

Figure 12 and 13 are plotted to evaluate the differences velocity profiles between $Al_2O_3 - H_2O$ and $Cu - H_2O$. Both graphs shown that when nanoparticles volume fraction rise, velocity profiles drop. It is due to the increment of the nanofluid viscosity which causes the nanofluid flow to slower down. Besides that, graph observation revealed $Al_2O_3 - H_2O$ has a greater velocity than $Cu - H_2O$. It is because Cu has higher density (8.92g/cm^3) compared to Al_2O_3 (3.95g/cm^3). Density of the nanoparticles affects the fluid's viscosity. Hence, fluid velocity consists of Cu slower than fluid consists ofAl_2O_3.

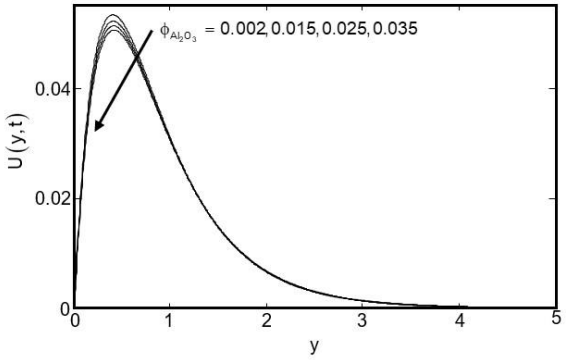

Fig. 12. Comparison of velocity profile for different values of $\varphi_{Al_2O_3}$, when $\varphi_{Cu} = 0.005$, $\lambda_1 = 1$, $\lambda = 1$, $Ha = 2$, $Q = 2$, $Pr = 6.2$, $Gr = 1.5$, $t = 1$, $Rd = 0.5$ and $Pr = 6.2$

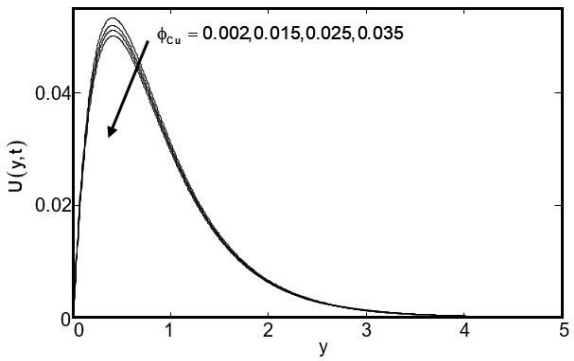

Fig. 13. Comparison of velocity profile for different values of φ_{Cu}, when $\varphi_{Al_2O_3} = 0.005$, $\lambda_1 = 1$, $\lambda = 1$, $Ha = 2$, $Q = 2$, $Pr = 6.2$, $Gr = 1.5$, $t = 1$, $Rd = 0.5$ and $Pr = 6.2$

Moreover, the influence of radiation on temperature field is plotted in Figure 14. As shown, higher values of Rd will increase the temperature distributions. This is because radiation effect signifies the relative contribution of conduction heat transfer to thermal radiation transfer. Figure 15 shows the effect of t on temperature profiles. It is clearly shown that temperature is an increasing function of t. This is because the temperature will increase as time increases due to a large amount of heat energy being released into the fluid.

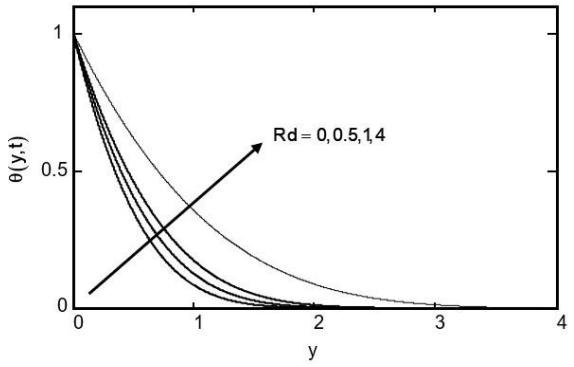

Fig. 14. Temperature profile for different value of Rd, when $Q = 0.5$, $Pr = 6.2$, $t = 1$ and $\varphi_{hnf} = 0.04$

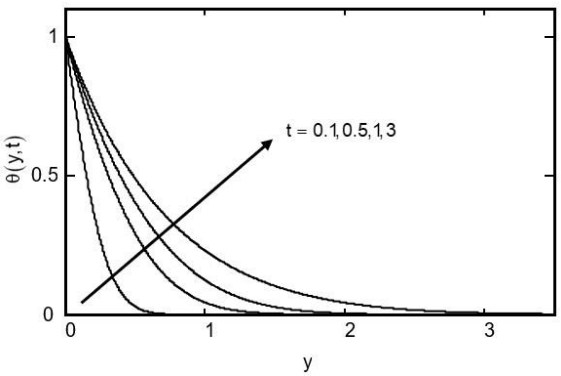

Fig. 15. Temperature profile for different value of t, when $Q = 0.5$, $Pr = 6.2$, $Rd = 0.5$ and $\varphi_{hnf} = 0.04$

The variation of heat absorption influence temperature profile is presented in Figure 16. It is found that, the behavior of parameter Q in temperature is like velocity profiles. It shown that the temperature decreases when heat absorption increases due to high viscous force in fluid flow which reduces the thermal energy of fluid. The effect of φ_{hnf} can been seen in Figure 17 and it is shown that, increase in φ_{hnf} will increase the temperature fields. The reason for this is that as more nanoparticles are added, the thermal conductivity of the nanofluid is improved, leading to an increase in the thermal boundary layer. This results in the dominance of thermal conduction in the flow and allows heat to diffuse rapidly from the heated surface, resulting in a high rate of heat transfer.

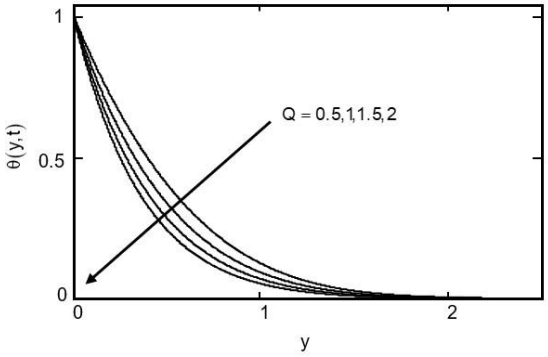

Fig. 16. Temperature profile for different value of Q, when $Rd = 0.5$, $Pr = 6.2$, $t = 1$ and $\varphi_{hnf} = 0.04$

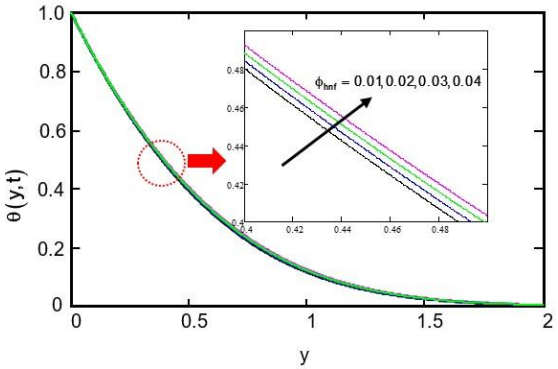

Fig. 17. Temperature profile for different value of φ_{hnf}, when $Rd = 0.5$, $Pr = 6.2$, $t = 1$ and $Q = 0.5$

The influence of Pr on temperature profiles is shown in Figure 18. Here, three physical values, $Pr = 6.2$ (water), $Pr = 21$ (Kerosene) and $Pr = 203$ (EG) have been chosen. As clearly shown, when Pr is increased, the temperature decreases. Prandtl number is the ratio of kinematic viscosity to thermal diffusivity. Therefore, when Pr is increased, the kinematic viscosity increases but thermal diffusivity decreases. Thus, temperature decreases due to the increase in kinematic viscosity.

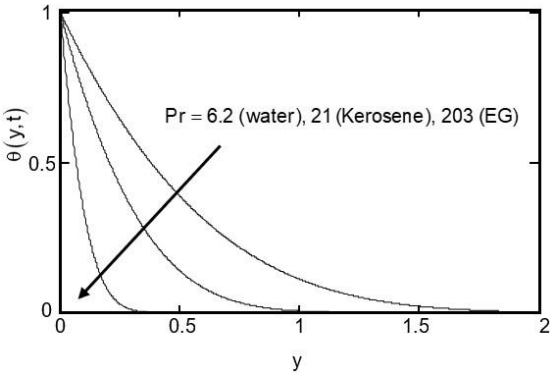

Fig. 18. Temperature profile for different value of Pr, when $Rd = 0.5$, $Q = 0.5$, $t = 1$ and $\varphi_{hnf} = 0.005$

Comparison of temperature profile for different nanofluids and regular Jeffrey fluid is also discussed in Figure 19. Physically, the addition of sufficient volume of nanoparticles leads to the enhancement of nanofluid's thermal conductivity. The more nanoparticles being inserted, the higher the thermal conductivity, which increases the temperature profiles. Besides, the results shown that, $Cu - H_2O$ is enhanced more heat energy compared to $Al_2O_3 - H_2O$ due to its properties which has higher thermal conductivity and heat diffusion. But both nanoparticles are still significantly enhancing the temperature profiles as can see in Figure 20 and 21.

The accuracy of the obtained solution is verified by comparing solution in Eq. (89) and (90) with the solution obtained by Khan [59] in Eq. (18) and (31). The comparison is conducted by letting nanoparticle volume fraction, thermal radiation, heat absorption and Hartmann number are equal to zero which are $\varphi_{hnf} = Rd = Q = Ha = 0$, respectively. This comparison shows the velocity and temperature profiles for both present and previous works are identical to each other as clearly presented in Figure 22 and 23, which thus proves that the accuracy of obtained solutions are verified and in excellent agreement. Meanwhile, another verification is also carried out to verify the validity of present solutions by comparing the values of both profiles from the present work by choosing $\varphi_{hnf} = 0$, and $\varphi_{hnf} = 0.04$. Physically, the addition of sufficient volume of nanoparticles leads to the enhancement of nanofluid's thermal conductivity. The more nanoparticles being inserted, the higher the thermal conductivity, which increases the velocity and temperature profiles.

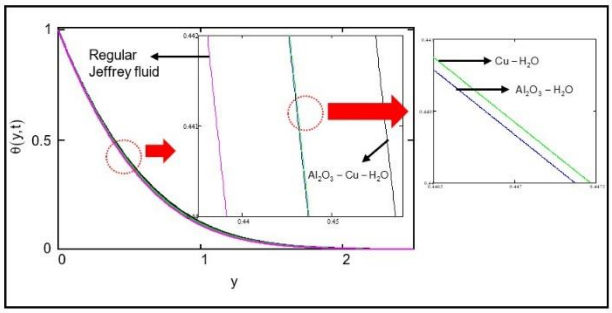

Fig. 19. Comparison of temperature profile for different nanofluids and regular Jeffrey fluid when, $Pr = 6.2$, $t = 1$, $Rd = 0.5$ and $Q = 0.5$

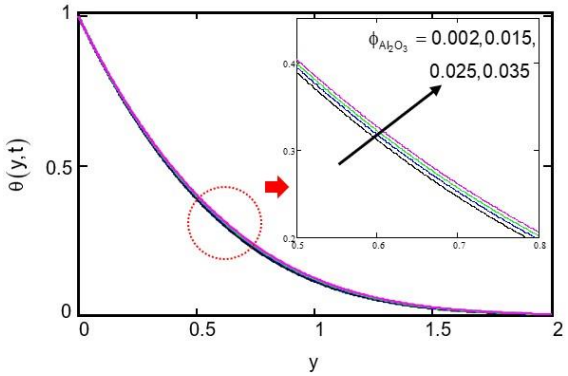

Fig. 20. Temperature profile for different value of $\varphi_{Al_2O_3}$, when $\varphi_{Cu} = 0.005$, $Pr = 6.2$, $t = 1$, $Rd = 0.5$ and $Q = 0.5$

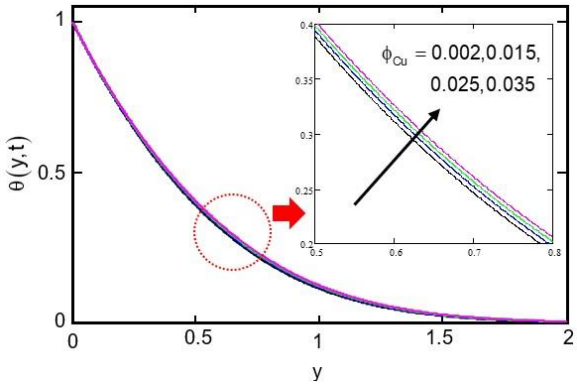

Fig. 21. Temperature profile for different value of φ_{Cu}, when $\varphi_{Al_2O_3} = 0.005$, $Pr = 6.2$, $t = 1$, $Rd = 0.5$ and $Q = 0.5$

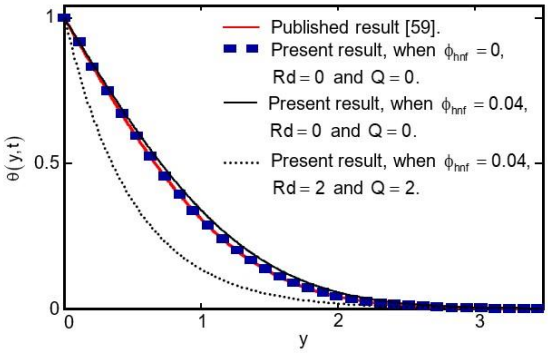

Fig. 22. Comparison of temperature profile in Eq. (36) and Eq. (89) with Eq. (18) by Khan [59], when $\Pr = 6.2$ and $t = 3$

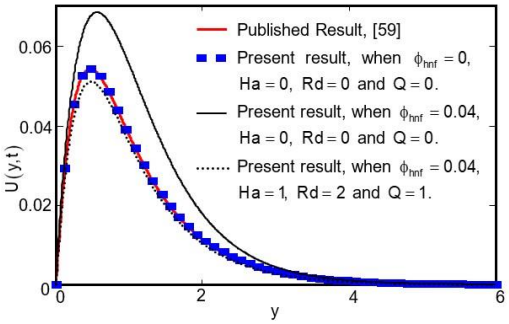

Fig. 23. Comparison of velocity profile in Eq. (64) and Eq. (90) with Eq. (31) published by Khan [59], when $\lambda_1 = \lambda = 0$, $Ha = 1$, $Gr = 1$, $\Pr = 6.2$ and $t = 1$

7. Conclusions

This article presented an analytical solution to an unsteady Jeffrey hybrid nanofluid with heat absorption and radiation effects. This problem is tackled by the Laplace transform method. The impacts of the embedded parameters on the Jeffrey hybrid nanofluid velocity and temperature are illustrated in graphs and discussed in detail. Moreover, the main findings from the discussion above are as follows:

i. The limiting case of the obtained result Eq. (89) and Eq. (90) are found in excellent mutual agreement with the previous study by Khan [59]. Thus, the accuracy of the obtained result is validated.
ii. Enhancement of the Jeffrey hybrid nanofluid velocity when Rd and Gr are increased.
iii. Jeffrey hybrid nanofluid velocity decreases as Q, Pr and φ_{hnf} increase.
iv. Temperature profiles increase when Rd, t and φ_{hnf} increase.
v. Interestingly, when $\lambda_1 = 0$, the present study can be reduced to unsteady free convection flow of MHD second grade hybrid nanofluid under influence of radiation and heat absorption effects as mentioned in Eq. (77).

The analysis of this analytical solution can be a reference for numerical and experimental works, as it could reduce the time and cost required to conduct an experiment as well as numerical study validation.

Acknowledgement
The authors extend their appreciation to Universiti Teknologi MARA for funding this work through "Geran Penyelidikan MyRA Lepasan PhD" under grant number 600-RMC/GPM LPHD 5/3 (141/2021).

References

[1] Choi, S. U. S., and Jeffrey A. Eastman. *Enhancing thermal conductivity of fluids with nanoparticles*. No. ANL/MSD/CP-84938; CONF-951135-29. Argonne National Lab.(ANL), Argonne, IL (United States), 1995.
[2] Hanif, Hanifa. "A finite difference method to analyze heat and mass transfer in kerosene based γ-oxide nanofluid for cooling applications." *Physica Scripta* 96, no. 9 (2021): 095215. https://doi.org/10.1088/1402-4896/ac098a
[3] Hanif, Hanifa, and Sharidan Shafie. "Interaction of multi-walled carbon nanotubes in mineral oil based Maxwell nanofluid." *Scientific Reports* 12, no. 1 (2022): 4712. https://doi.org/10.1038/s41598-022-07958-y
[4] Hanif, Hanifa, and Sharidan Shafie. "Impact of Al_2O_3 in electrically conducting mineral oil-based maxwell nanofluid: application to the petroleum industry." *Fractal and Fractional* 6, no. 4 (2022): 180. https://doi.org/10.3390/fractalfract6040180
[5] Saeed, Aamir, R. Ali Shah, M. Sohail Khan, Unai Fernandez-Gamiz, Mutasem Z. Bani-Fwaz, Samad Noeiaghdam, and Ahmed M. Galal. "Theoretical analysis of unsteady squeezing nanofluid flow with physical properties." *Mathematical Biosciences and Engineering* 19, no. 10 (2022): 10176-10191. https://doi.org/10.3934/mbe.2022477
[6] Sharma, Madhu, Bhupendra K. Sharma, Umesh Khanduri, Nidhish K. Mishra, Samad Noeiaghdam, and Unai Fernandez-Gamiz. "Optimization of heat transfer nanofluid blood flow through a stenosed artery in the presence of Hall effect and hematocrit dependent viscosity." *Case Studies in Thermal Engineering* 47 (2023): 103075. https://doi.org/10.1016/j.csite.2023.103075
[7] Sharma, Bhupendra K., Chandan Kumawat, and Muhammad Mubashir Bhatti. "Optimizing energy generation in power-law nanofluid flow through curved arteries with gold nanoparticles." *Numerical Heat Transfer, Part A: Applications* (2023): 1-33. https://doi.org/10.1080/10407782.2023.2232123
[8] Mishra, Nidhish K., Madhu Sharma, B. K. Sharma, and Umesh Khanduri. "Soret and Dufour effects on MHD nanofluid flow of blood through a stenosed artery with variable viscosity." *International Journal of Modern Physics B* (2023): 2350266. https://doi.org/10.1142/S0217979223502661
[9] Ghadikolaei, S. S., M. Yassari, H. Sadeghi, Kh Hosseinzadeh, and D. D. Ganji. "Investigation on thermophysical properties of TiO_2-Cu/H_2O hybrid nanofluid transport dependent on shape factor in MHD stagnation point flow." *Powder Technology* 322 (2017): 428-438. https://doi.org/10.1016/j.powtec.2017.09.006
[10] Sarkar, Jahar, Pradyumna Ghosh, and Arjumand Adil. "A review on hybrid nanofluids: recent research, development and applications." *Renewable and Sustainable Energy Reviews* 43 (2015): 164-177. https://doi.org/10.1016/j.rser.2014.11.023
[11] Sidik, Nor Azwadi Che, Isa Muhammad Adamu, Muhammad Mahmud Jamil, G. H. R. Kefayati, Rizalman Mamat, and G. Najafi. "Recent progress on hybrid nanofluids in heat transfer applications: a comprehensive review." *International Communications in Heat and Mass Transfer* 78 (2016): 68-79. https://doi.org/10.1016/j.icheatmasstransfer.2016.08.019
[12] Babu, J. A. Ranga, K. Kiran Kumar, and S. Srinivasa Rao. "State-of-art review on hybrid nanofluids." *Renewable and Sustainable Energy Reviews* 77 (2017): 551-565. https://doi.org/10.1016/j.rser.2017.04.040
[13] Hayat, Tanzila, and S. Nadeem. "Heat transfer enhancement with Ag-CuO/water hybrid nanofluid." *Results in Physics* 7 (2017): 2317-2324. https://doi.org/10.1016/j.rinp.2017.06.034
[14] Salleh, Siti Nur Alwani, Norfifah Bachok, Fadzilah Md Ali, and Norihan Md Arifin. "Flow and wall heat transfer due to a continuously moving slender needle in hybrid nanofluid with stability analysis." *Journal of Advanced Research in Fluid Mechanics and Thermal Sciences* 76, no. 3 (2020): 62-74. https://doi.org/10.37934/arfmts.76.3.6274
[15] Hussain, Azad, Mohammed Hamed Alshbool, Aishah Abdussattar, Aysha Rehman, Hijaz Ahmad, Taher A. Nofal, and M. Riaz Khan. "A computational model for hybrid nanofluid flow on a rotating surface in the existence of convective condition." *Case Studies in Thermal Engineering* 26 (2021): 101089. https://doi.org/10.1016/j.csite.2021.101089
[16] Hanif, Hanifa, and Sharidan Shafie. "Application of Cattaneo heat flux to Maxwell hybrid nanofluid model: a numerical approach." *The European Physical Journal Plus* 137, no. 8 (2022): 989. https://doi.org/10.1140/epjp/s13360-022-03209-1

[17] Dinarvand, Saeed, Mahmoud Behrouz, Salar Ahmadi, Parsa Ghasemi, Samad Noeiaghdam, and Unai Fernandez-Gamiz. "Mixed convection of thermomicropolar AgNPs-GrNPs nanofluid: An application of mass-based hybrid nanofluid model." *Case Studies in Thermal Engineering* (2023): 103224. https://doi.org/10.1016/j.csite.2023.103224

[18] Hanif, Hanifa, Liaquat Ali Lund, Rahimah Mahat, and Sharidan Shafie. "Heat transfer analysis of Maxwell hybrid nanofluid with fractional Cattaneo heat flux." *Alexandria Engineering Journal* 72 (2023): 545-557. https://doi.org/10.1016/j.aej.2023.04.022

[19] Sharma, Bhupendra K., Parikshit Sharma, Nidhish K. Mishra, Samad Noeiaghdam, and Unai Fernandez-Gamiz. "Bayesian regularization networks for micropolar ternary hybrid nanofluid flow of blood with homogeneous and heterogeneous reactions: Entropy generation optimization." *Alexandria Engineering Journal* 77 (2023): 127-148. https://doi.org/10.1016/j.aej.2023.06.080

[20] Sharma, B. K., R. Gandhi, T. Abbas, and M. M. Bhatti. "Magnetohydrodynamics hemodynamics hybrid nanofluid flow through inclined stenotic artery." *Applied Mathematics and Mechanics* 44, no. 3 (2023): 459-476. https://doi.org/10.1007/s10483-023-2961-7

[21] Sharma, Bhupendra K., Parikshit Sharma, Nidhish K. Mishra, and Unai Fernandez-Gamiz. "Darcy-Forchheimer hybrid nanofluid flow over the rotating Riga disk in the presence of chemical reaction: Artificial neural network approach." *Alexandria Engineering Journal* 76 (2023): 101-130. https://doi.org/10.1016/j.aej.2023.06.014

[22] Kamis, Nur Ilyana, Noraihan Afiqah Rawi, Lim Yeou Jiann, Sharidan Shafie, and Mohd Rijal Ilias. "Thermal Characteristics of an Unsteady Hybrid Nano-Casson Fluid Passing Through a Stretching Thin-Film with Mass Transition." *Journal of Advanced Research in Fluid Mechanics and Thermal Sciences* 104, no. 2 (2023): 36-50. https://doi.org/10.37934/arfmts.104.2.3650

[23] Ali, Zaileha Md, Nur Zahidah Ismail, Mohd Rijal Ilias, Siti Khuzaimah Soid, Anuar Ishak, Md Faisal Md Basir, and Nur Hazirah Adilla Norzawary. "Hyperbolic Tangent Fluid Model for Stagnation Flow of Hybrid Nanofluid Over a Stretching Sheet." *Journal of Advanced Research in Fluid Mechanics and Thermal Sciences* 107, no. 1 (2023): 87-101. https://doi.org/10.37934/arfmts.107.1.87101

[24] Zukri, Norsyasya Zahirah Mohd, Mohd Rijal Ilias, Siti Shuhada Ishak, Roselah Osman, Nur Asiah Mohd Makhatar, and Mohd Nashriq Abd Rahman. "Magnetohydrodynamic Effect in Mixed Convection Casson Hybrid Nanofluids Flow and Heat Transfer over a Moving Vertical Plate." *CFD Letters* 15, no. 7 (2023): 92-111. https://doi.org/10.37934/cfdl.15.7.92111

[25] Fetecau, Corina, M. Jamil, Constantin Fetecau, and I. Siddique. "A note on the second problem of Stokes for Maxwell fluids." *International Journal of Non-Linear Mechanics* 44, no. 10 (2009): 1085-1090. https://doi.org/10.1016/j.ijnonlinmec.2009.08.003

[26] Vieru, Dumitru, Corina Fetecau, and Constantin Fetecau. "Flow of a viscoelastic fluid with the fractional Maxwell model between two side walls perpendicular to a plate." *Applied Mathematics and Computation* 200, no. 1 (2008): 459-464. https://doi.org/10.1016/j.amc.2007.11.017

[27] Vieru, Dumitru, and Abdul Rauf. "Stokes flows of a Maxwell fluid with wall slip condition." *Canadian Journal of Physics* 89, no. 10 (2011): 1061-1071. https://doi.org/10.1139/p11-099

[28] Dunn, J. E., and K. R. Rajagopal. "Fluids of differential type: critical review and thermodynamic analysis." *International Journal of Engineering Science* 33, no. 5 (1995): 689-729. https://doi.org/10.1016/0020-7225(94)00078-X

[29] Galdi, Giovanni Paolo, and Jindrich Necas. *Recent developments in theoretical fluid mechanics*. CRC Press, 1993.

[30] Sharma, B. K., Anup Kumar, Rishu Gandhi, and M. M. Bhatti. "Exponential space and thermal-dependent heat source effects on electro-magneto-hydrodynamic Jeffrey fluid flow over a vertical stretching surface." *International Journal of Modern Physics B* 36, no. 30 (2022): 2250220. https://doi.org/10.1142/S0217979222502204

[31] Awais, Muhammad, Huma Rehman, Muhammad Asif Zahoor Raja, Saeed Ehsan Awan, Aamir Ali, Muhammad Shoaib, and Muhammad Yousaf Malik. "Hall effect on MHD Jeffrey fluid flow with Cattaneo-Christov heat flux model: An application of stochastic neural computing." *Complex & Intelligent Systems* 8, no. 6 (2022): 5177-5201. https://doi.org/10.1007/s40747-022-00754-1

[32] Hussain, Zakir, Ashraf Hussain, Muhammad Shoaib Anwar, and Muhammad Farooq. "Analysis of Cattaneo-Christov heat flux in Jeffery fluid flow with heat source over a stretching cylinder." *Journal of Thermal Analysis and Calorimetry* 147, no. 4 (2022): 3391-3403. https://doi.org/10.1007/s10973-021-10573-0

[33] Kumar, Anup, Bhupendra K. Sharma, Rishu Gandhi, Nidhish K. Mishra, and M. M. Bhatti. "Response surface optimization for the electromagnetohydrodynamic Cu-polyvinyl alcohol/water Jeffrey nanofluid flow with an exponential heat source." *Journal of Magnetism and Magnetic Materials* 576 (2023): 170751. https://doi.org/10.1016/j.jmmm.2023.170751

[34] Mishra, Nidhish K., Bhupendra K. Sharma, Parikshit Sharma, Taseer Muhammad, and Laura M. Pérez. "Entropy generation optimization of cilia regulated MHD ternary hybrid Jeffery nanofluid with Arrhenius activation energy

and induced magnetic field." *Scientific Reports* 13, no. 1 (2023): 14483. https://doi.org/10.1038/s41598-023-41299-8

[35] Saraswathi, H., Shreedevi Kalyan, and Ali J. Chamkha. "Steady of Thermal and Concentration Effect on a Fully Developed Jeffrey Fluid with Baffle in a Vertical Passage." *Journal of Nanofluids* 12, no. 2 (2023): 341-347. https://doi.org/10.1166/jon.2023.2001

[36] Sharma, Bhupendra Kumar, Anup Kumar, Rishu Gandhi, Muhammad Mubashir Bhatti, and Nidhish Kumar Mishra. "Entropy generation and thermal radiation analysis of EMHD Jeffrey nanofluid flow: Applications in solar energy." *Nanomaterials* 13, no. 3 (2023): 544. https://doi.org/10.3390/nano13030544

[37] Krishna, M. Veera, K. Bharathi, and Ali J. Chamkha. "Hall effects on MHD peristaltic flow of Jeffrey fluid through porous medium in a vertical stratum." *Interfacial Phenomena and Heat Transfer* 6, no. 3 (2018). https://doi.org/10.1615/InterfacPhenomHeatTransfer.2019030215

[38] Krishna, M. Veera, B. V. Swarnalathamma, and Ali J. Chamkha. "Investigations of Soret, Joule and Hall effects on MHD rotating mixed convective flow past an infinite vertical porous plate." *Journal of Ocean Engineering and Science* 4, no. 3 (2019): 263-275. https://doi.org/10.1016/j.joes.2019.05.002

[39] Krishna, M. Veera, and Ali J. Chamkha. "Hall and ion slip effects on Unsteady MHD Convective Rotating flow of Nanofluids-Application in Biomedical Engineering." *Journal of the Egyptian Mathematical Society* 28, no. 1 (2020): 1. https://doi.org/10.1186/s42787-019-0065-2

[40] Amar, N., and N. Kishan. "The influence of radiation on MHD boundary layer flow past a nano fluid wedge embedded in porous media." *Partial Differential Equations in Applied Mathematics* 4 (2021): 100082. https://doi.org/10.1016/j.padiff.2021.100082

[41] Khashi'ie, Najiyah Safwa, Norihan Md Arifin, and Ioan Pop. "Magnetohydrodynamics (MHD) boundary layer flow of hybrid nanofluid over a moving plate with Joule heating." *Alexandria Engineering Journal* 61, no. 3 (2022): 1938-1945. https://doi.org/10.1016/j.aej.2021.07.032

[42] Sharma, B. K., and Rishu Gandhi. "Combined effects of Joule heating and non-uniform heat source/sink on unsteady MHD mixed convective flow over a vertical stretching surface embedded in a Darcy-Forchheimer porous medium." *Propulsion and Power Research* 11, no. 2 (2022): 276-292. https://doi.org/10.1016/j.jppr.2022.06.001

[43] Reddy, Yanala Dharmendar, Bejawada Shankar Goud, Nagi Reddy Nalivela, and Vempati Srinivasa Rao. "Impact of porosity on two-dimensional unsteady MHD boundary layer heat and mass transfer stagnation point flow with radiation and viscous dissipation." *Numerical Heat Transfer, Part A: Applications* (2023): 1-19. https://doi.org/10.1080/10407782.2023.2198739

[44] Sharma, Pawan K., Bhupendra K. Sharma, Nidhish K. Mishra, and Harshini Rajesh. "Impact of Arrhenius activation energy on MHD nanofluid flow past a stretching sheet with exponential heat source: A modified Buongiorno's model approach." *International Journal of Modern Physics B* (2023): 2350284. https://doi.org/10.1142/S0217979223502843

[45] Bestman, A. R., and S. K. Adjepong. "Unsteady hydromagnetic free-convection flow with radiative heat transfer in a rotating fluid: I. Incompressible optically thin fluid." *Astrophysics and Space Science* 143 (1988): 73-80. https://doi.org/10.1007/BF00636756

[46] Roşca, Natalia C., Alin V. Roşca, and Ioan Pop. "Axisymmetric flow of hybrid nanofluid due to a permeable non-linearly stretching/shrinking sheet with radiation effect." *International Journal of Numerical Methods for Heat & Fluid Flow* 31, no. 7 (2021): 2330-2346. https://doi.org/10.1108/HFF-09-2020-0574

[47] Ali, Liaqat, Ye Wang, Bagh Ali, Xiaomin Liu, Anwarud Din, and Qasem Al Mdallal. "The function of nanoparticle's diameter and Darcy-Forchheimer flow over a cylinder with effect of magnetic field and thermal radiation." *Case Studies in Thermal Engineering* 28 (2021): 101392. https://doi.org/10.1016/j.csite.2021.101392

[48] Bejawada, Shankar Goud, Yanala Dharmendar Reddy, Wasim Jamshed, Kottakkaran Sooppy Nisar, Abdulaziz N. Alharbi, and Ridha Chouikh. "Radiation effect on MHD Casson fluid flow over an inclined non-linear surface with chemical reaction in a Forchheimer porous medium." *Alexandria Engineering Journal* 61, no. 10 (2022): 8207-8220. https://doi.org/10.1016/j.aej.2022.01.043

[49] Wang, Yinyin, R. Naveen Kumar, Soumaya Gouadria, Maha M. Helmi, RJ Punith Gowda, Essam Roshdy El-Zahar, B. C. Prasannakumara, and M. Ijaz Khan. "A three-dimensional flow of an Oldroyd-B liquid with magnetic field and radiation effects: An application of thermophoretic particle deposition." *International Communications in Heat and Mass Transfer* 134 (2022): 106007. https://doi.org/10.1016/j.icheatmasstransfer.2022.106007

[50] Guedri, Kamel, Zafar Mahmood, Bandar M. Fadhl, Basim M. Makhdoum, Sayed M. Eldin, and Umar Khan. "Mathematical analysis of nonlinear thermal radiation and nanoparticle aggregation on unsteady MHD flow of micropolar nanofluid over shrinking sheet." *Heliyon* 9, no. 3 (2023). https://doi.org/10.1016/j.heliyon.2023.e14248

[51] Zainal, Nurul Amira, Iskandar Waini, Najiyah Safwa Khashi'ie, Abdul Rahman Mohd Kasim, Kohilavani Naganthran, Roslinda Nazar, and Ioan Pop. "Stagnation point hybrid nanofluid flow past a stretching/shrinking sheet driven by

Arrhenius kinetics and radiation effect." *Alexandria Engineering Journal* 68 (2023): 29-38. https://doi.org/10.1016/j.aej.2023.01.005

[52] Mohana, C. M., and B. Rushi Kumar. "Nanoparticle shape effects on hydromagnetic flow of Cu-water nanofluid over a nonlinear stretching sheet in a porous medium with heat source, thermal radiation, and Joule heating." ZAMM-Journal of Applied Mathematics and Mechanics/Zeitschrift für Angewandte Mathematik und Mechanik (2023): e202300188. https://doi.org/10.1002/zamm.202300188

[53] Maheswari, Chundru, Ravuri Mohana Ramana, Shaik Mohiddin Shaw, G. Dharmaiah, and S. Noeiaghdam. "Numerical investigation on MHD forchheimer flow of Fe_3O_4-H_2O, Cu-H_2O and Ag-H_2O nanofluids over permeable stretching sheet with radiation." *Results in Engineering* (2023): 101194.

[54] Khanafer, Khalil, Kambiz Vafai, and Marilyn Lightstone. "Buoyancy-driven heat transfer enhancement in a two-dimensional enclosure utilizing nanofluids." *International Journal of Heat and Mass Transfer* 46, no. 19 (2003): 3639-3653. https://doi.org/10.1016/S0017-9310(03)00156-X

[55] Gul, Aaiza, Ilyas Khan, Sharidan Shafie, Asma Khalid, and Arshad Khan. "Heat transfer in MHD mixed convection flow of a ferrofluid along a vertical channel." *PloS One* 10, no. 11 (2015): e0141213. https://doi.org/10.1371/journal.pone.0141213

[56] Turkyilmazoglu, M., and I. Pop. "Heat and mass transfer of unsteady natural convection flow of some nanofluids past a vertical infinite flat plate with radiation effect." *International Journal of Heat and Mass Transfer* 59 (2013): 167-171. https://doi.org/10.1016/j.ijheatmasstransfer.2012.12.009

[57] Ghara, N., S. Das, S. L. Maji, and R. N. Jana. "Effect of radiation on MHD free convection flow past an impulsively moving vertical plate with ramped wall temperature." *American Journal of Scientific and Industrial Research* 3, no. 6 (2012): 376-386. https://doi.org/10.5251/ajsir.2012.3.6.376.386

[58] Tiwari, Raj Kamal, and Manab Kumar Das. "Heat transfer augmentation in a two-sided lid-driven differentially heated square cavity utilizing nanofluids." *International Journal of Heat and Mass Transfer* 50, no. 9-10 (2007): 2002-2018. https://doi.org/10.1016/j.ijheatmasstransfer.2006.09.034

[59] Khan, Ilyas. "A note on exact solutions for the unsteady free convection flow of a Jeffrey fluid." *Zeitschrift für Naturforschung A* 70, no. 6 (2015): 397-401. https://doi.org/10.1515/zna-2015-0010

[60] Zin, Nor Athirah Mohd, Ilyas Khan, and Sharidan Shafie. "The impact silver nanoparticles on MHD free convection flow of Jeffrey fluid over an oscillating vertical plate embedded in a porous medium." *Journal of Molecular Liquids* 222 (2016): 138-150. https://doi.org/10.1016/j.molliq.2016.06.098

[61] Krishna, M. Veera. "Chemical reaction, heat absorption and Newtonian heating on MHD free convective Casson hybrid nanofluids past an infinite oscillating vertical porous plate." *International Communications in Heat and Mass Transfer* 138 (2022): 106327. https://doi.org/10.1016/j.icheatmasstransfer.2022.106327

[62] Saqib, Muhammad, Ilyas Khan, and Sharidan Shafie. "Application of fractional differential equations to heat transfer in hybrid nanofluid: modeling and solution via integral transforms." *Advances in Difference Equations* 2019, no. 1 (2019): 1-18. https://doi.org/10.1186/s13662-019-1988-5

[63] Roy, Nepal Chandra, and Ioan Pop. "Exact solutions of Stokes' second problem for hybrid nanofluid flow with a heat source." *Physics of Fluids* 33, no. 6 (2021). https://doi.org/10.1063/5.0054576

[64] Sandeep, N., V. Sugunamma, and P. Mohankrishna. "Effects of radiation on an unsteady natural convective flow of a EG-Nimonic 80a nanofluid past an infinite vertical plate." *Advances in physics Theories and Applications* 23 (2013): 36-43.

[65] Zulkiflee, Fasihah, Sharidan Shafie, and Ahmad Qushairi Mohamad. "Unsteady Free Convection Flow of Nanofluids between Vertical Oscillating Plates with Mass Diffusion." *Journal of Advanced Research in Fluid Mechanics and Thermal Sciences* 76, no. 2 (2020): 118-131. https://doi.org/10.37934/arfmts.76.2.118131

[66] Jamshed, Wasim, Nor Ain Azeany Mohd Nasir, Siti Suzilliana Putri Mohamed Isa, Rabia Safdar, Faisal Shahzad, Kottakkaran Sooppy Nisar, Mohamed R. Eid, Abdel-Haleem Abdel-Aty, and I. S. Yahia. "Thermal growth in solar water pump using Prandtl-Eyring hybrid nanofluid: a solar energy application." *Scientific Reports* 11, no. 1 (2021): 18704. https://doi.org/10.1038/s41598-021-98103-8

[67] Cortell, R. "Fluid flow and radiative nonlinear heat transfer over a stretching sheet." *Journal of King Saud University-Science* 26, no. 2 (2014): 161-167. https://doi.org/10.1016/j.jksus.2013.08.004

[68] Pantokratoras, Asterios, and Tiegang Fang. "Sakiadis flow with nonlinear Rosseland thermal radiation." *Physica Scripta* 87, no. 1 (2012): 015703. https://doi.org/10.1088/0031-8949/87/01/015703

[69] Nazar, M., Corina Fetecau, D. Vieru, and C. Fetecau. "New exact solutions corresponding to the second problem of Stokes for second grade fluids." *Nonlinear Analysis: Real World Applications* 11, no. 1 (2010): 584-591. https://doi.org/10.1016/j.nonrwa.2008.10.055

[70] Hetnarski, Richard B. "An algorithm for generating some inverse Laplace transforms of exponential form." *Zeitschrift für angewandte Mathematik und Physik ZAMP* 26 (1975): 249-253. https://doi.org/10.1007/BF01591514